Marine Pollution Bulletin 154 (2020) 111092

Contents lists available at ScienceDirect

Marine Pollution Bulletin

journal homepage: www.elsevier.com/locate/marpolbul

Microplastic accumulation in deep-sea sediments from the Rockall Trough

Winnie Courtene-Jones[a,*], Brian Quinn[b], Ciaran Ewins[b], Stefan F. Gary[a], Bhavani E. Narayanaswamy[a]

[a] Scottish Association for Marine Science, Scottish Marine Institute, Oban, Argyll, PA37 1QA, Scotland, United Kingdom
[b] Institute of Biomedical and Environmental Health Research (IBEHR), School of Science & Sport, University of the West of Scotland, Paisley, PA1 2BE, Scotland, United Kingdom

ARTICLE INFO

Keywords:
Microplastic
Pollution
Deep-sea
Plastic
Sediment record
Chronology

ABSTRACT

Microplastics are widely dispersed through the marine environment. Few studies have assessed the long-term or historic prevalence of microplastics, yet acquiring such data can inform their distribution, transport and the environmental risks posed. To quantify the distribution and polymer types temporally, sediment cores were collected from > 2000 m water depth in the Rockall Trough, North Atlantic Ocean. As hypothesized, a significant negative trend was observed in the frequency of microplastics with increasing sediment age, however there was an increase in polymer diversity. Microplastics were pervasive throughout the sediment analysed (10 cm depth), yet lead-210 (^{210}Pb) activities were confined to the upper 4 cm, indicating this layer to be ~150 years old and thus the presence of microplastics far exceed the production of modern plastic. A number of mechanisms, including sediment reworking, could redistribute microplastics vertically. Additionally, microplastics abundance was significantly correlated with sediment porosity, suggesting interstitial transport via pore waters.

1. Introduction

The pollution of sediments with microplastics is a widespread and global phenomenon (Barnes et al., 2009; Browne et al., 2011). The majority of studies have focused on beaches and coastal areas (reviewed in Van Cauwenberghe et al., 2015), however recent studies have documented the presence of microplastics on the seafloor at bathyal, abyssal and hadal depths (Bergmann et al., 2017; Fischer et al., 2015; Jamieson et al., 2019; Peng et al., 2018; Woodall et al., 2014). Despite these reports, the global extent and quantities of microplastics on the deep seafloor remains largely unknown.

In the marine environment, microplastics will likely develop biofilms and aggregate quickly with organic material (Michels et al., 2018; Porter et al., 2018; Summers et al., 2018), which modifies the density of those particles and may facilitate their sinking to the seafloor. Due to the low oxygen levels, cold temperature, lack of ultraviolet radiation and often low energy regimes typically found in the deep benthic zone, the breakdown of plastics are much slower than compared to the terrestrial environment or sea surface (Andrady, 2011). A thorough assessment of the prevalence of microplastics on the seafloor is necessary not only to consider their long-term behaviour and explore whether this is an accumulation site for microplastics, as has been hypothesized (Kanhai et al., 2019; Woodall et al., 2014) but also to assess the fluxes of plastic reaching the seabed which can better inform plastic mass balance models (Hardesty et al., 2017; Kane and Clare, 2019; Koelmans et al., 2017) and consider their bioavailability to the benthic community. Numerous benthic species are reported to ingest microplastics (Bour et al., 2018; Courtene-Jones et al., 2017; Graham and Thompson, 2009; Taylor et al., 2016), but as yet the ambient concentrations they are exposed to and their impacts remain unclear.

Long-term datasets of macro/microplastics on the seafloor are sparse (Courtene-Jones et al., 2019; Maes et al., 2018) and in the absence of such monitoring the analysis of environmental archives, such as sediment cores offer a means to investigate temporal changes. Indeed, sediment cores have widely been used to assess the deposition and historical occurrence of various pollutants (Boonyatumanond et al., 2007; Bryan and Langston, 1992; Van Metre and Mahler, 2005) and more recently have been utilized to study microplastics in coastal areas (Claessens et al., 2011; Matsuguma et al., 2017; Willis et al., 2017) and freshwater lakes (Turner et al., 2019). However the same temporal analysis is lagging when considering the deep-marine environment.

Radionuclides offer a widely-used tool to estimate the age of sediments and have broad application including in the study of sediment dynamics, palaeoclimatic conditions and anthropogenic induced

* Corresponding author.
E-mail address: Winnie.courtene-jones@plymouth.ac.uk (W. Courtene-Jones).

https://doi.org/10.1016/j.marpolbul.2020.111092
Received 1 December 2019; Received in revised form 18 March 2020; Accepted 18 March 2020
Available online 26 March 2020

changes (Kirchner, 2011). One such isotope is lead-210 (^{210}Pb) which is a naturally occurring radioactive form of lead. ^{210}Pb falls out of the atmosphere and once in the air-sea interface it is quickly removed onto suspended particulate matter and deposited to the seafloor (MacKenzie et al., 2011). As a consequence the accumulation and burial of sediments, with co-contaminant radioactive decay, is assumed to produce a vertical distribution of ^{210}Pb with a systematic decrease in activity as a function of depth. Due to the short half-life of ^{210}Pb ($t_{1/2}$ = ~22 years) (Komárek et al., 2008) this tracer is widely used to investigate recent events occurring over the last 100–150 years (Appleby, 2008; Arias-Ortiz et al., 2018), a resolution which aligns well with the mass production of modern plastics and thus provides a suitable method to study historic microplastic deposition.

The study aimed to quantify the abundance and polymer composition of microplastics through depth-sectioned sediment cores collected from > 2000 m water depth in the North East Atlantic Ocean. It was hypothesized that there would be a negative trend in the abundance of microplastics through the core profile, i.e. with increasing sediment chronology. The age of the sediment was inferred using radioisotope analysis with the aim of detecting the onset and historic prevalence of microplastics in this region. Finally, sediment characteristics such as water content, porosity, particle grain size and organic matter content were analysed to explore the relationships between these variables and the deposition of microplastics.

2. Method

2.1. Sampling location

The Rockall Trough is situated to the west of Scotland, United Kingdom. The monitoring site 'Gage Station M' is located in the Rockall Trough (57.300°N, −10.383° W) at a depth of 2200 m. During the 2017 research cruise DY78–79 on-board *R.R.S. Discovery*, three megacorer deployments were carried out within the locality of Gage Station M (Fig. 1 and Supplementary information). Megacorers are designed to sample without creating a bow-wave and thus ensure sediments are not disturbed (Jamieson et al., 2013).

2.2. Quality assurance/quality control (QA/QC)

QA/QC was implemented wherever possible while on board the research cruise. Core tubes and rubber bungs were rinsed with deionised water prior to their use. The core collar, stainless steel cutter and spatula used to section the sediment cores were also washed thoroughly between use to prevent sample contamination or cross-contamination. Personnel wore nitrile gloves and where possible wore cotton coveralls, however due to weather limitations sometimes waterproof outwear was required. Samples of putative contaminants, such as the ropes used on the megacorer, tubes and bungs as well as clothing were taken to be analysed alongside the microplastics samples.

Within the laboratory, thorough cleaning of work benches and laboratory equipment was undertaken prior to any work. Glass and metal laboratory equipment were preferentially used over plastic and consumables were used directly from sterile packaging. Equipment was kept covered with clean aluminium foil when not in use and the samples were covered as much as possible to minimize exposure risk. Tape-lift screening and atmospheric controls to monitor background contamination were implemented as detailed in Courtene-Jones et al., (2017).

2.3. Megacorer deployments and sediment processing

An OSIL megacorer was utilized to obtain sediment cores from three sites around Gage Station M (details in Supplementary information). The megacorer was rigged with six 60 cm long x 10 cm wide internal diameter core tubes to allow for a 50% redundancy. Sampling followed the guidelines outlined by Narayanaswamy et al. (2016), which are summarized in the Supplementary information.

Once on deck the core tubes were carefully removed from the megacorer frame and sealed with pre-cleaned rubber bungs at each end, before being transferred to wooden stands. The supernatant water from each of the sediment cores was carefully siphoned off so as not to disturb any of the underlying sediment. Each core (A – C) was sliced using a stainless steel cutter at discrete depth intervals; 0.5 cm sections were taken for the uppermost 5 cm of sediment, 1 cm intervals between the depths of 5–10 cm, and 5 cm sections were taken thereafter until the end of the core. The extrusion of cores can lead to smearing effects at the outer edges (Chant and Cornett, 1987), thus a few millimetres from the edges of each core section were removed with a stainless steel spatula to avoid mixing artefacts caused by this process. Sediment horizons were transferred to labelled clean polyethylene zip lock bags, sealed immediately and frozen at −20 °C for later analysis of microplastic concentrations.

2.4. Laboratory methods

2.4.1. Extraction of microplastics from sediment cores

The entire mass of sediment obtained from each depth horizon from the cores A and C from each of the three megacorer deployments (MG1697, MG1678, MG1699) were assessed for microplastics. Cores were processed in a random order to prevent bias in this extraction phase. Sediments were freeze dried and the weight of each horizon was recorded prior to processing. Microplastics were extracted from the sediment using the oil extraction protocol (Crichton et al., 2017), with slight modifications to account for the larger sediment masses and smaller grain sizes analysed here than in the original method.

Dry sediment ranged in weight from 9 g to 79.6 g; samples with a large mass (> 40 g) were divided and two separate extractions were carried out. These samples (maximum 40 g dry weight (d.w.)) were put into separate pre-cleaned 250 ml conical flasks and double the volume of deionised water was added. For subsamples > 25 g d.w., 7 ml of canola oil was added to this, while 5 ml of canola oil was added to sediment (sub)samples weighing < 25 g d.w. which was indicated from preliminary experiments using spiked sediment samples. An aluminium foil lid was placed onto the conical flask and the contents were swirled for 30 s. This was then transferred to a 100 ml borosilicate glass separating funnel. The conical flask was rinsed twice with 25 ml of deionised water to ensure no particles remained on the internal walls and this was decanted into the separating funnel. The separating funnel was mixed vigorously for 30 s and then left to settle for 30 min. Following the settling period, the sediment and aqueous layers were emptied from the separating funnel into a waste beaker. A further 30 ml of deionised water was added to the separating funnel and it again was shaken vigorously for 30 s. This was then left for a second settling period of 30 min before the aqueous layer containing remaining sediment grains were emptied from the funnel into the waste beaker.

The oil layer was retained and vacuum filtered through a 52 μm mesh size disc of transparent nylon gauze. The separating funnel was rinsed twice with 20 ml of 4% non-foaming detergent (Alcojet, Sigma-Aldrich) to remove any oil and remaining particles, this was then emptied through the gauze filter. The gauze was transferred to a lidded glass petri dish and was examined thoroughly three times under a dissecting microscope (Wild M5). Potential microplastics were transferred to a 30 mm petri dish containing a disc of filter paper (Whatman No. 1). To remove the oil residue from the surface of the microplastics a mixture of 99% ethanol and 99% isopropanol in a 1:1 ratio was used. Microplastics specific to each sample, were transferred to a glass cavity block in which a 5 ml volume of the ethanol:propanol mixture had been added. This was covered and incubated for 15 min, before the microplastics were recovered from the solvent mixture and returned to their specific 30 mm petri dish and sealed for further analysis.

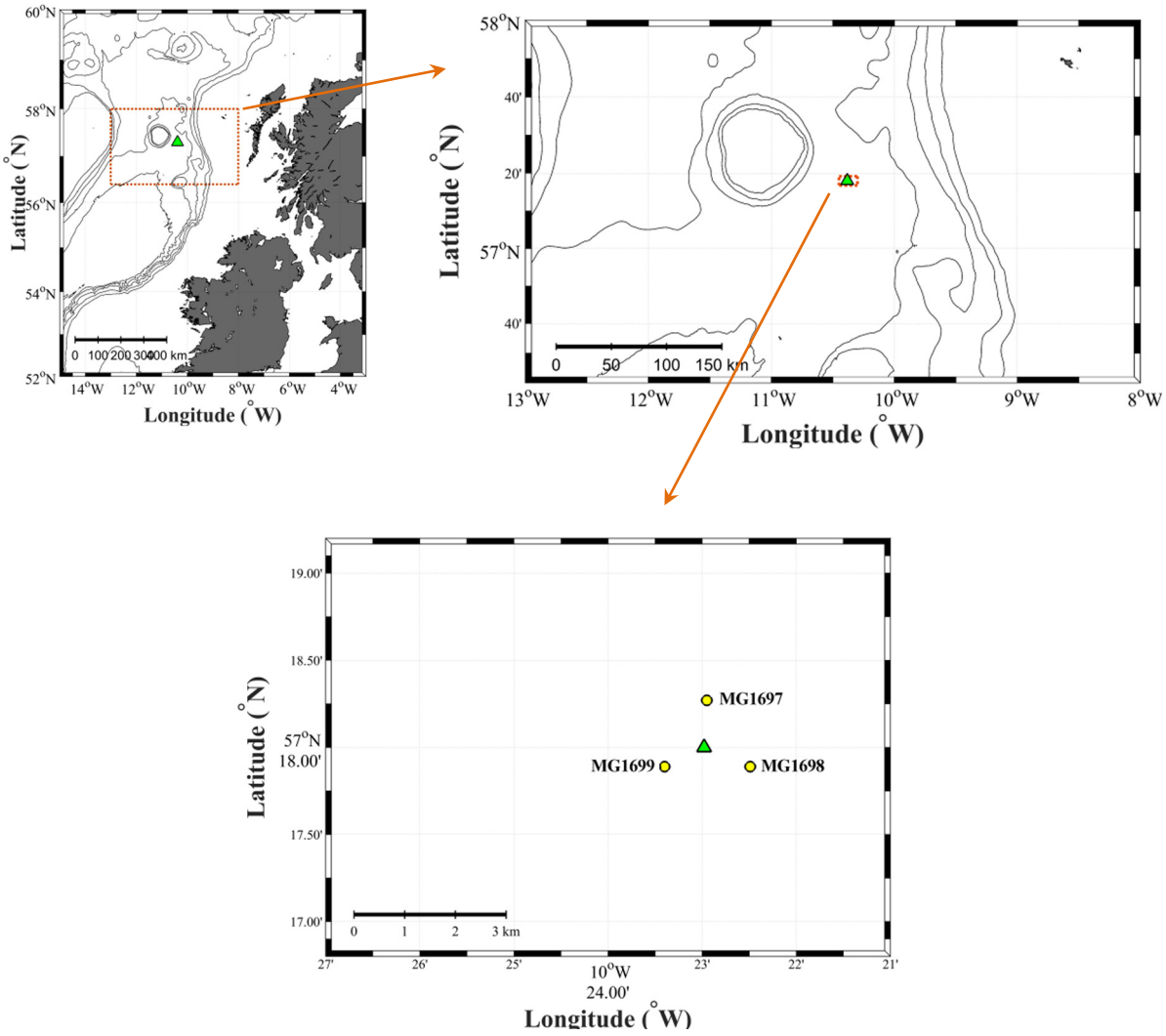

Fig. 1. The location of the three megacorer deployments (yellow points, n = 3) around Gage Station M (green triangle). The area depicted inside the box is shown in the subsequent panel. (For interpretation of the references to color in this figure legend, the reader is referred to the web version of this article.)

2.4.2. Identification of microplastics

The length of each microplastic particle was measured visually using the ocular scale of a Wild M5 dissecting microscope. Putative microplastics were analysed with a Perkin-Elmer One Fourier Transformation infrared (FTIR) microscope in transmission mode. Infrared radiation in the wavenumbers 600–4000 cm^{-1} were used and each spectra produced was the average from 16 co-added scans and was corrected against a background scan carried out prior to each sample. A variable aperture size was used and the spectral resolution was 4 cm^{-1}. Data were visualized in OMNIC 9 (Thermo Fisher Scientific Inc.) with use of the inbuilt Hummel polymer library and the Alfred Wegener Institute 'AWI' (Primpke et al., 2018) library to facilitate polymeric identification; additionally, the characteristic functional group signals from each spectra were manually examined.

2.4.3. Radiometric dating of sediment cores

Dried sediment samples from core MG1697 B were analysed for 210-lead (^{210}Pb), 226-Radium (^{226}Ra), Caesium-137 (^{137}Cs) and Americium-241 (^{241}Am) by direct gamma assay at the Environmental Radiometric Facility, University College London, using an ORTEC HPGe GWL series well-type coaxial low background intrinsic germanium detector. ^{210}Pb was determined via its gamma emissions at 46.5 keV, and ^{226}Ra by the 295 keV and 352 keV gamma rays emitted by its daughter isotope ^{214}Pb following three weeks of storage in sealed containers to allow radioactive equilibration. The characteristic emissions at 662 keV and 59.5 keV were measured for ^{137}Cs and ^{241}Am respectively (Appleby et al., 1986). The absolute efficiencies of the detector were determined using calibrated sources and sediment samples of known activity. Corrections were made for the effect of self-absorption of low energy gamma rays within the sample (Appleby et al., 1992).

2.4.4. Sediment particle size analysis

Sediment samples from core B from each of the three deployments (MG1697, MG1698, MG1699) were utilized for particle grain size analysis. Each sample depth (0–10 cm) was physically homogenized for one minute with a clean stainless steel spatula, before 5 g wet weight sub-samples was transferred to individual sterile zip-lock bags and freeze-dried. The freeze-dried material was transferred to individual falcon tubes to which 5 ml of 0.2% sodium hexametaphosphate (Calgon) dispersant and 20 ml of deionised water was added to prevent particle coagulation. Samples were mixed on a vortex mixer set at 2500 rpm for one minute. Immediately prior to analysis the sediment sample was vortex mixed and grain size analysis was preformed using a Beckman Coulter LS230 laser diffraction device equipped with sonicator. The software GRADISTAT V8 (Blott and Pye, 2001) was used for the geometric classification of the sediment based on the Folk and Ward method (Folk and Ward, 1957).

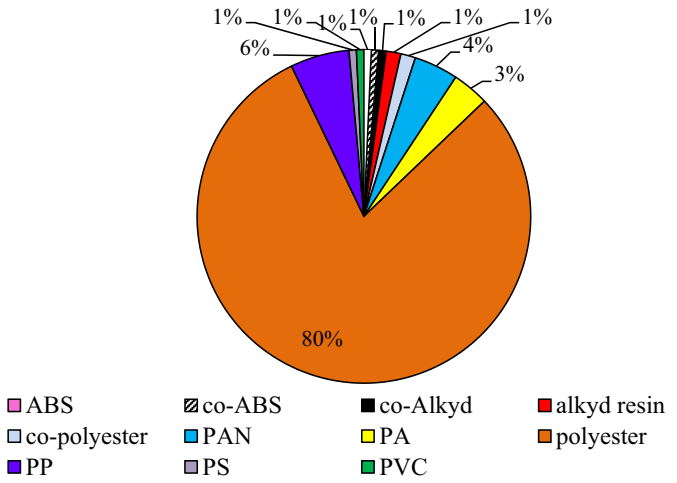

Fig. 2. The proportions, as percentages, of microplastic polymers found throughout the sediment profile, (co-ABS = acrylonitrile butadiene styrene copolymer; co-polyester = polyester copolymer; ABS = acrylonitrile butadiene styrene; PVC = polyvinyl chloride; PAN = polyacrylonitrile; co-alkyd = alkyd copolymer; PP = polypropylene; PS = polystyrene; PA = polyamide). (For interpretation of colour, the reader is referred to the web version of this article.)

2.4.5. Particulate organic carbon and nitrogen

Freeze dried sediment from each of the depth horizons (0–10 cm) from core MG1697 B were placed into separate agate pots and ground for 3 min at 350 rpm in a ball mill grinder. Representative ground subsamples (in the range 25–30 mg) were transferred to 2 ml glass ampoule and were weighed to four decimal places. Each of the sample depths were analysed in triplicate. To each ampoule, 1 ml of sulphurous acid (5–6%) was added to remove the calcium carbonate portion of the sample. The samples were left to degas for 8 h and were then stored under vacuum in a desiccator overnight, before being freeze-dried. The contents of each ampoule were transferred into separate tin capsules, ensuring no sediment remained on the internal walls of the glass vials. The samples were then combusted using an EAS Costech 4020 Elemental Combustion Analyser at 950 °C in an oxygen rich atmosphere, which momentarily causes the temperature to rise to 1600 °C. The Elemental Combustion Analyser was calibrated by analysing a series of Acetanilide carbon-nitrogen standards, and a spirulina standard and the medium organic content soil standard, B2178, were also run in parallel with the sediment samples to monitor recovery. The limit of detection was calculated using 3 × 1 SD of the mean of the blank data.

2.4.6. Water content and porosity

The volume of water and the percentage water content of each sediment sample were calculated. From this the bulk density of sediment and sediment porosity could be calculated using the equations in the Supplementary information.

2.5. Statistical analysis

Microplastics were counted and normalised by the sediment dry weight (MP/g d.w.) Data were tested for normality and homogeneity of variance using the Shapiro-Wilk and Bartlett tests, and were $\log_{10}$ transformed where necessary to meet these criteria. All analyses were performed in R studio V 1.1.383 (R Core Team, 2016), with the use of the packages ggplot2 (Wichkham and Chang, 2016), permute (Simpson et al., 2016), lattice (Sarkar, 2018) and vegan (Oksanen et al., 2018).

2.5.1. Analysis of microplastic abundance and polymer types across depth and the relationship to environmental variables

To investigate the relationship between sediment depth and the number of MP/g d.w. sediment Pearson's correlation coefficient were used. Microplastics were grouped into size classes of 0.5 mm intervals and Pearson's correlation coefficient was computed to identify the relationship between microplastics size and abundance. To investigate differences in the abundance of polymer types across sampling depths a one-way analysis of variance (ANOVA) was utilized for $\log_{10}$ transformed polyester data. Data for polyacrylonitrile (PAN) and polypropylene (PP) failed to meet the criteria for parametric statistics, therefore Kruskal-Wallis H tests were used for these polymers. Other polymers were not present in sufficient numbers to perform this analysis.

Finally, to consider the relationship between microplastic abundance and environmental data, namely sediment porosity, particulate organic carbon (POC) and particulate organic nitrogen (PON), a series of Person correlation coefficients were computed.

2.5.2. Analysis of polymer diversity

The Shannon-Weiner diversity index (H′) was utilized to compute the diversity of polymers at different sediment depths and the relationship between the diversity index and sediment depth was examined with Pearson's correlation coefficient.

3. Results

3.1. Quantifying microplastics in the sediment cores

3.1.1. Microplastic identification and characterization

Of the 361 putative microplastics that were analysed with FTIR, 140 were identified as synthetic polymeric material (39%), 180 as natural material (50%), and 16 yielded unusable spectra (4%). Additionally, 24 particles (7%) could not be scanned due to problems transferring them to the gold slide owing to their small size, or they were lost (electrostatic charges can cause particles to be repelled from the slides), and one particle could not be assigned to a material based on its FTIR spectrum. All microplastics were secondary in their origin, either fibres (n = 124, 89%), fragments (n = 14, 10%), or pieces of film (n = 2, 1%) with no spheroids or pellets present; examples are shown in the Supplementary information.

A total of 11 synthetic polymers were identified, polyester was the most abundant constituting 80% of the polymeric material, followed by polypropylene (6%) (Fig. 2). A number of copolymers were also identified, e.g. co-alkyd, co-ABS and co-polyester, these materials had distinct spectral peaks corresponding to alkyd, ABS and polyester respectively, however additional peaks were also present indicating the presence of other monomer units/polymers, hence their classification as co-polymers (Scott and Penlidis, 2017).

Microplastic particles ranged in size from 0.06 mm to > 12 mm (Fig. 3). Smaller particle sizes were most abundant and 90% of the confirmed microplastic particles were smaller than 2.5 mm in diameter. By grouping particle sizes into 0.5 mm intervals, a significant negative correlation was identified between the abundance of microplastics and their increasing size (Pearson's p, $r = -0.778$, $p = 0.001$).

3.1.2. Microplastic abundance across sediment depths

Microplastics were found to be pervasive in all sediment cores and present down to a depth of 10 cm, the maximum depth examined within this study. The greatest abundance of microplastic/g d.w. was in the top 0.5 cm (mean ± SD: 0.197 ± 0.129 MP/g d.w.) and the lowest abundance occurred at a depth of 8–9 cm (mean ± SD: 0.197 ± 0.129 MP/g d.w.) (Fig. 4). A significant negative trend was observed between sediment depth and the number of microplastics isolated (Pearson's p, $r = -0.420$, $p \leq 0.001$).

Variation was observed in the abundance of microplastic polymers across the sediment depth profile (Fig. 5). Polyester was ubiquitous to all sediment depths; however others, such as ABS, PS and PVC were only contained within a single depth interval (7–8 cm, 2.5–3 cm,

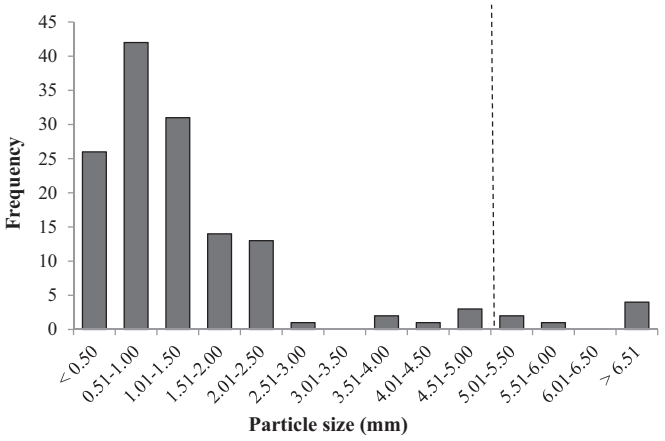

Fig. 3. Size distribution of microplastic particles isolated from the sediment cores.

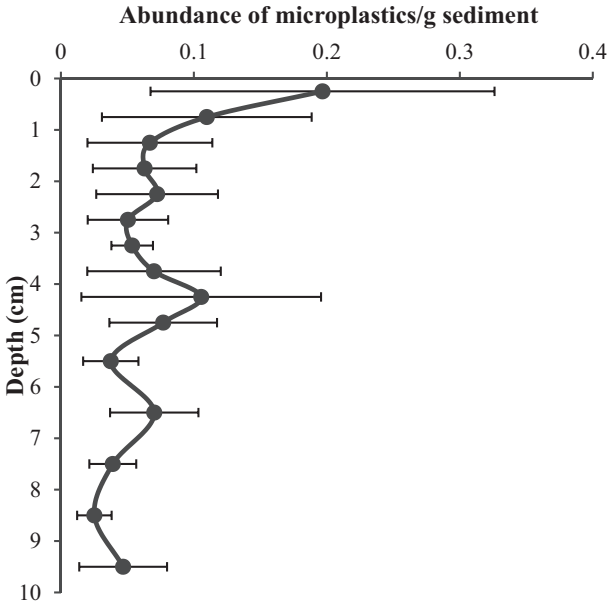

Fig. 4. The mean abundance of microplastics/g dry weight (d.w.) sediment at each depth interval averaged across all sediment cores (n = 6); error bars show standard deviation.

0–0.5 cm, respectively). To further investigate these intra-polymer differences across sampling depth, analysis of variance was performed. No statistical differences were found in the abundance of microplastic/g d.w. between sampling depth for PP (H = 3.8, df = 3, p = 0.284) or PAN (H = 4.857, df = 4, p = 0.302). Statistically significant differences were apparent however when analysing the abundance of polyester/g d.w. sediment (F = 2.32, df = 14, p = 0.018); explained by a significant difference between its abundance at 8–9 cm and 0–0.5 cm depth (p = 0.002) (Fig. 5).

Computing polymer diversities, based on the Shannon Weiner diversity index (H′), for each dry sediment horizon yielded unexpected results (Fig. 6). The polymer diversity was found to be greatest in the top 0.5 cm of sediment (H′ = 1.357), however, overall a positive but not significant trend was observed in the polymer diversity with increasing depth (Pearson's p, r = 0.364, p = 0.182).

3.2. Radiometric dating

3.2.1. ^{210}Pb activity

The equilibrium depth of total ^{210}Pb activity with supported ^{210}Pb

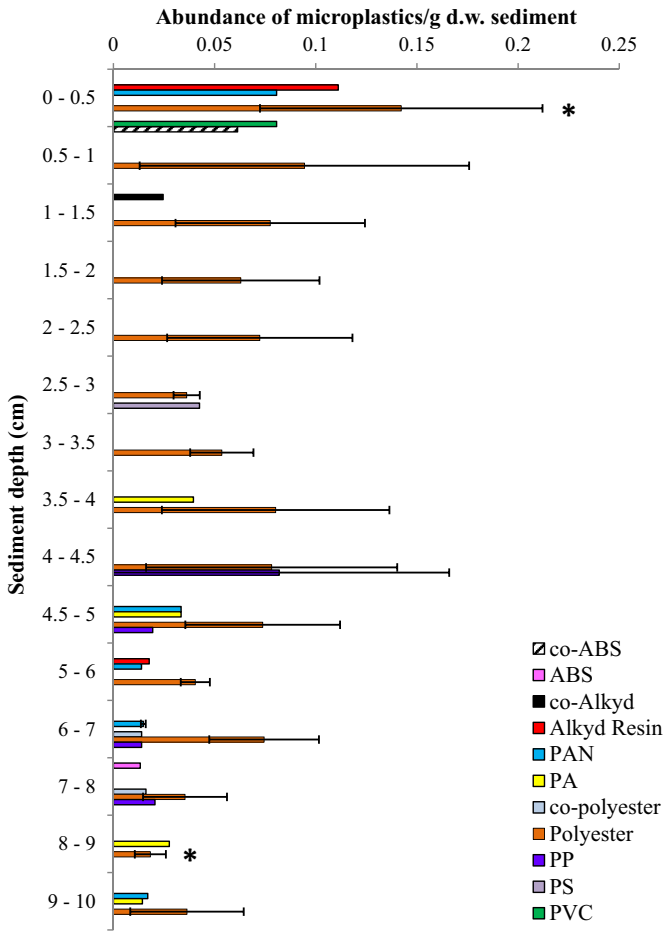

Fig. 5. The mean abundance of polymer types per gram of dry weight sediment across the sediment profile for all cores (n = 6). Error bars show standard deviation and the star indicates significant differences (p = ≤ 0.05) between quantities. (co-ABS = acrylonitrile butadiene styrene copolymer; co-polyester = polyester copolymer; ABS = acrylonitrile butadiene styrene; PVC = polyvinyl chloride; PAN = polyacrylonitrile; co-alkyd = alkyd copolymer; PP = polypropylene; PS = polystyrene; PA = polyamide).(For interpretation of colour, the reader is referred to the web version of this article.)

activity is reached at ~5.0 cm of the core MG1697 B. Unsupported ^{210}Pb activities, calculated by subtracting ^{226}Ra activity (as supported ^{210}Pb) from total ^{210}Pb activity, decline more or less exponentially with depth in the top 3.0 cm sediments suggesting relatively uniform sedimentation rates. However, below this depth the decline in activity departs from the exponential trend, implying changes in the sedimentation rates (Supplementary Information).

3.2.2. Artificial fallout radionuclides

Detectable ^{137}Cs activity was present at a depth of 2.5 cm and a low ^{241}Am activity was also detected in the surface sediment, at a depth of 0.5 cm (Supplementary Information). These signals may be derived from the fallout of atmospheric testing of nuclear weapons which was at its maximum level in 1963 (Hu et al., 2010; Warwick et al., 2001). There is a mismatch in the sediment depths from which signals of these artificial radionuclides were detected. However the peak of ^{137}Cs at a depth of 2.5 cm supports the ^{210}Pb derived core chronologies presented below.

3.2.3. Core chronology

Irregular changes in unsupported ^{210}Pb activities of the core precluded the use of the constant initial concentration (CIC) dating model and instead the ^{210}Pb chronologies were calculated using the constant

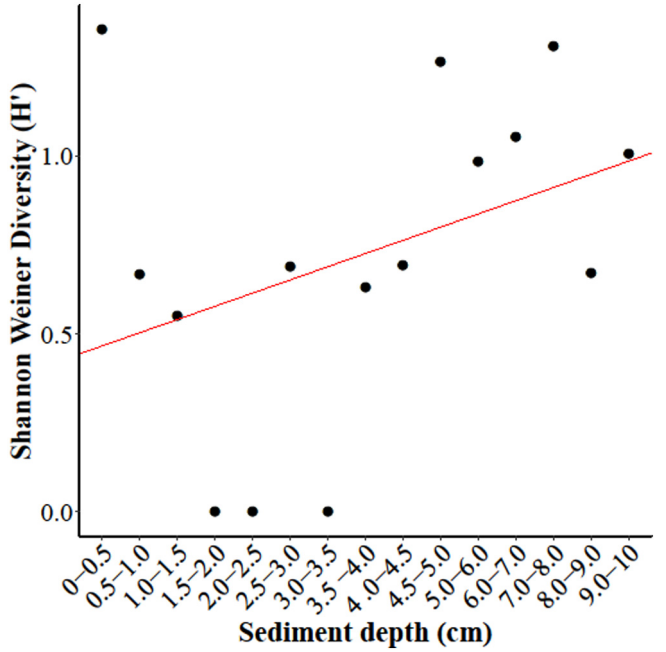

Fig. 6. The diversity of polymers, based on the calculated Shannon Weiner diversity index (H′) calculated from the abundance of microplastics polymers/g d.w. across sediment depths. The red line shows the linear regression between the two variables. (For interpretation of the references to color in this figure legend, the reader is referred to the web version of this article.)

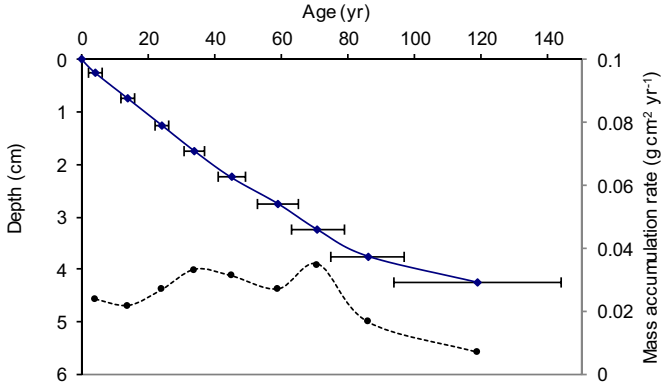

Fig. 7. Radiometric chronology of core MG1697 B, showing the CRS model ^{210}Pb dates in years, depicted by the solid line with error bars denoting standard deviation, and the mass accumulation rate of sediment (g cm^{-2} y^{-1}) is shown by the dashed line.

rate of ^{210}Pb supply (CRS) dating model (Appleby, 2001; Appleby and Oldfield, 1978). The sedimentation rate varied from 0.009 cm y^{-1}, to 0.055 cm y^{-1}, with mass accumulation rate increasing from 0.007 g cm^{-2} y^{-1} in the deeper layers (4.25 cm depth which was dated to the 1890s), to a peak of 0.0348 g cm^{-2} y^{-1} at a depth of 3.25 cm (dated from the mid-1940s) (Fig. 7). Through the top 3.25 cm there was little change in sedimentation rates. Simple calculations based on the sedimentation rate and the commencement of mass plastic production in the 1940s, indicates that plastics should only be present to a maximum depth of 4 cm; which is supported by the ^{210}Pb derived chronologies.

3.3. Particle grain size

Using the geometric grain size obtained from the Folk and Ward sediment classification system, the major sediment type from each of the megacorer deployments was 'sandy silt'. Grain size remained relatively consistent throughout the core (Supplementary Information) and there was little particle size sorting across the depth profile, indicated by sorting values (σ_I) of 1.77–2.83, where values of > 4 indicate extremely poorly sorted, and < 0.5 indicate well sorted sediments.

3.4. Particulate organic carbon and nitrogen

Carbon is buried in sediments in the form of particulate organic carbon (POC), here the profile is typical for that of deep sediments (Gehlen et al., 1997; Suess, 1980). As expected, the percentage weight of POC is highest in the surface layers indicating newly deposited sediments, thereafter POC decreases with depth before an increase and plateau is observed between 7 and 10 cm (Supplementary Information). Overall POC content was low and accounted for 0.54–0.37% of the sediment dry weight. Particulate organic nitrogen (PON) decays faster than POC in the environment and so values for PON are lower, overall PON accounted for 0.03–0.14% of the sediment dry weight. PON displays a more complex pattern than POC, whereby enrichment is noted at a depth of ~2 cm, and a gradual increase is observed between 7 and 10 cm (Supplementary Information).

3.5. Water content and porosity of the sediment

The water content decreases across the depth profile (Supplementary Information), as expected. Porosity shows a more irregular pattern, however a general trend of decreasing porosity with increasing depth is observed (Supplementary information) as particles are consolidated.

3.6. Relationship between microplastics abundance and environmental variables

The environmental variables POC, PON and sediment porosity were investigated to explore their relationship with the abundance of microplastics. No correlation was found between the abundance of microplastics and PON (Pearson's p, $r = -0.132$, p = 0.639) or POC (Pearson's p, $r = 0.388$, p = 0.153). A significant positive relationship was identified between microplastics abundance and sediment porosity (Pearson's p $r = 0.672$, p = 0.006) (Fig. 8).

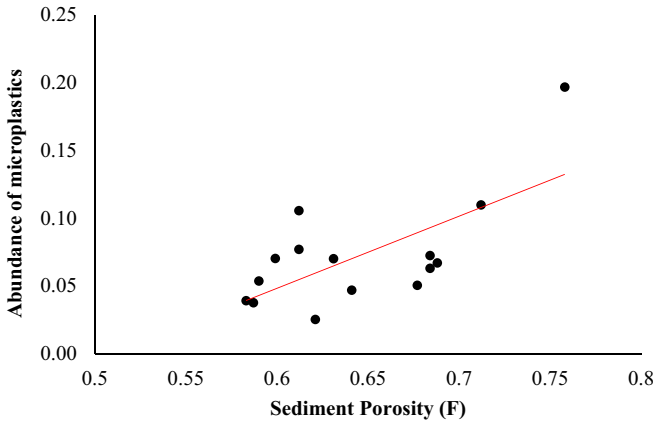

Fig. 8. The relationship between sediment porosity and the mean abundance of microplastics. The red line shows the relationship between the two variables. (For interpretation of the references to color in this figure legend, the reader is referred to the web version of this article.)

4. Discussion

4.1. The distribution of microplastics throughout the sediment profile

Microplastics were documented throughout the upper 10 cm of the sediment core which was the maximum depth investigated in this study. The majority of published studies have only considered microplastic pollution within superficial sediments (Alomar et al., 2016; Stolte et al., 2015; Van Cauwenberghe et al., 2013). When comparing the quantities enumerated from the uppermost layer, the data from the Rockall Trough (0.196 MP g^{-1} in the top 0.5 cm) are similar to those reported in coastal sediments (Claessens et al., 2011; Clunies-Ross et al., 2016; Frias et al., 2016), but are lower than those in deep Arctic sediments (up to 6595 MP/kg (Bergmann et al., 2017)). Such variability in concentrations could indicate the heterogeneous spatial distribution of microplastics on the deep seafloor or may have arisen through analytical differences between the studies. Bergmann et al., (2017) report an exponential increase in the number of microplastics with decreasing size, and in the Arctic sediments they studies, 99% of the microplastics were $<$ 150 μm in size. In this study, small microplastics may not have been adequately captured due to the 52 μm filter size used, and thus, based on the findings of Bergmann et al., (2017) the abundance reported here is likely an under-estimation.

Microplastic concentrations varied between the sediment horizons and as hypothesized a significant negative trend was identified between the abundance of microplastics and increasing depth through the core profile corresponding to older sediments. A similar trend is reported in other studies from coastal to deep ocean environments (Brandon et al., 2019; Claessens et al., 2011; Martin et al., 2017; Matsuguma et al., 2017; Willis et al., 2017) corroborating these findings. In each of these studies the maximum burial depth of microplastics varied, this will depend partly on sedimentation rate, which differs widely between locations. In the North Atlantic the sedimentation rate is 4.4–6.5 cm kyr^{-1} (Thomson et al., 2000), therefore based on this and the duration of plastic manufacture, it was expected that microplastics would be located within the top few centimetres of the sediment core only. This estimate was supported by the spike in the radioisotope ^{137}Cs, located at a depth of ~2.5 cm. ^{137}Cs is derived from human nuclear activity and due to the peak in nuclear weapons testing in 1960, a maximum of ^{137}Cs is generally observed in sediments corresponding to the year 1963 (Hong et al., 2011) and in turn provides a method to date modern sediments. The spike in ^{137}Cs activity indicates sediments located shallower than a depth of 2.5 cm have been deposited within the last ~50 years, a timescale corresponding to the mass production of plastics.

^{210}Pb activities were detected to a maximum depth of ~4.5 cm, estimating these sediments to be from the year 1898 ± 25, long predating the production of plastics. Based on the radioisotope analyses carried out, it was therefore unexpected to find plastics distributed throughout the core. Some care is needed when interpreting chronologies derived from ^{210}Pb data, as a number of assumptions are made within the dating models (Appleby and Oldfield, 1978; Arias-Ortiz et al., 2018), however the dates generated from the two independent radionuclides (^{137}Cs and ^{210}Pb) agree, giving confidence to the data. Unsupported ^{210}Pb activities declined more or less exponentially through the uppermost 3.5 cm of sediment, whereupon the signal departed from this exponential trend. This could suggest variation in the sedimentation rate but more likely indicates the presence of localised physical/biological mixing (Arias-Ortiz et al., 2018).

Most particles that sink to the seafloor are displaced a few times by fauna prior to their more or less permanent burial (Wheatcroft, 1992). Benthic species interact with the upper layers of sediment during feeding and movement and on a global scale sediment mixing occurs to a depth of 5.75 ± 4.67 cm (Teal et al., 2008). In the Feni drift, a region of the Rockall Trough to the south-west of Gage Station M, the surface mixed layer was recorded to a maximum depth of 14–16 cm and to a depth of 17 cm on Rockall Bank (Thomson et al., 2000). This may be attributed to the presence of large burrowing species from the taxonomic groups Sipuncula, Echiuria and Aplacophora which live at depth inside burrows and can contribute to sediment reworking and the drawing down of organic matter (Haywood and Ryland, 1990; Hughes et al., 2005). The benthic ecology at Gage Station M has long been studied (Gage, 1986) and an abundant and diverse infaunal community is present which is numerically dominated by polychaetes (Davies et al., 2006; Gage, 1986; Gage et al., 1980). As such, bioturbation is present within this region (Howe, 1995; Masson et al., 2002) and some evidence of burrows were observed within some of the sediment cores used in this study. The ability of benthic organisms to transport microplastics through sediment profiles have been demonstrated in the laboratory (Lwanga et al., 2017; Näkki et al., 2017), however by its very nature bioturbation causes sediment mixing which does not align with the discrepancy between the persistence of microplastics throughout the profile while the confinement of ^{210}Pb in the upper 4 cm. ^{210}Pb adsorbs to the charged sites on sediment grains and therefore if sediment reworking was responsible for distributing microplastics to a depth of 10 cm, ^{210}Pb activity would also be expected at this depth.

Redistribution of microplastics could occur by means of internal waves, however this process would also cause the transport and sorting of sediments, which is not supported by the particle size analysis which remains relatively consistent throughout the profile. Generally locations dominated by fine grained sediments are areas where there is little effect of bottom currents and therefore limited sediment transportation, i.e. these regions are relatively static, which is upheld by the well-studied physical oceanography of the Rockall Trough (Holliday et al., 2015).

A further explanation is offered through the analysis of the sediment properties. While no correlation was identified between the number of microplastics and the organic matter content of sediments as reported in previously (Alomar et al., 2016), a significant positive relationship was identified between sediment porosity and microplastics abundance, indicating that microplastics may be re-distributed within pore waters. Porosity is expected to decrease as a function of depth due to the consolidation of sediment particles (Reimers et al., 1992). While a general decrease is observed over the sediment core, sediment lying at a depth of 3 cm show a sharp reduction in their porosity and a gradual increase is observed between 8 and 10 cm. The majority of the microplastics identified were fibres, it is possible that due to their dimensions (long and thin) they behave in a different way to microplastic particles and may be transported between sediment grains carried within pore waters. Meiofauna inhabit the interstitial spaces between sediment grains and are abundant within deep-sea ecosystems (Ramirez-Llodra et al., 2010), including in the Rockall Trough (Davies et al., 2006; Paterson and Lambshead, 1995). These organisms displace sediment grains as they move and feed, and therefore based on their functional traits could further influence the vertical distribution of microplastics, however further work is required to assess this.

4.2. Polymer composition

Utilising FTIR spectroscopy, a diverse range of synthetic polymers (n = 11) were identified within the sediment cores (total sediment analysed amounted to 4710 cm^3/3.67 kg). Polyester was ubiquitous to all sampling depths and supports the widespread and prevalent occurrence of this polymer in environmental samples (Barrows et al., 2018; Browne et al., 2011; Courtene-Jones et al., 2019, 2017; Sanchez-Vidal et al., 2018). The majority of polymers were distributed more sporadically through the core, however PVC was confined only to the uppermost 0.5 cm, and polyamide and polypropylene were only present deeper than 3.5 cm and 4 cm respectively. Due to the low number of particles recovered of each polymer type more meaningful data are presented when considering the entire polymer 'community' at each

depth interval. Polymer diversity, based on the Shannon Weiner index (H′), was highest in the uppermost half centimetre of sediment. This is not surprising, as freshly deposited material collects here, indicated by the higher POC and PON values. Interestingly, while not significant, there was an overall positive trend observed between polymer diversity with increasing depth; a pattern not identified in previous coring studies (Martin et al., 2017; Matsuguma et al., 2017).

The majority of the polymeric material had densities greater than seawater, such as polyester, polyamide, PVC, PAN and alkyd resin; these high density polymers are found extensively within sediments worldwide (Bergmann et al., 2017; Browne et al., 2011). Here, non-expanded PS (1.04 g cm^{-3}) and ABS (1–1.1 g cm^{-3}) which are neutral or only slightly denser than seawater and also the positively buoyant polymer PP (0.8 g cm^{-3}) were isolated between 0 and 7 cm depth, however no pattern was found between depth and the buoyant polymers.

Author contributions

WCJ and BN conceptualised the study. WCJ participated in field sampling, undertook laboratory work and data analysis. CE contributed spectroscopy expertise and use of the FTIR. WCJ wrote the manuscript which received comments from all co-authors.

Funding

WCJ was jointly funded through a PhD scholarship awarded by the University of the Highlands and Island and the Scottish Association for Marine Science. SG was supported by NERC National Capability funding (R8-H12-85).

Declaration of competing interest

The authors declare that the research was conducted in the absence of any commercial or financial relationships that could be construed as a potential conflict of interest.

Acknowledgments

Thanks are extended to Dr. Handong Yang at the University College London Environmental Radiometric Facility for performing radionuclide analyses; to the captain, crew and researchers of the DY078-79 cruise for their assistance in sample collection and to Colin Abernethy and Dr. Richard Abel for their advice and assistance on sediment analysis.

Appendix A. Supplementary data

Supplementary data to this article can be found online at https://doi.org/10.1016/j.marpolbul.2020.111092.

References

Alomar, C., Estarellas, F., Deudero, S., 2016. Microplastics in the Mediterranean Sea: deposition in coastal shallow sediments, spatial variation and preferential grain size. Mar. Environ. Res. 115, 1–10. https://doi.org/10.1016/j.marenvres.2016.01.005.

Andrady, A.L., 2011. Microplastics in the marine environment. Mar. Pollut. Bull. 62, 1596–1605. https://doi.org/10.1016/j.marpolbul.2011.05.030.

Appleby, P.G., 2001. Chronostratigraphic techniques in recent sediments. In: Last, W.M., Smol, J.P. (Eds.), Tracking Environmental Change Using Lake Sediments. Vol. 1: Basin Analysis, Coring, and Chronological Techniques. Kluwer Academic Publishers, Dordrecht, pp. 171–203.

Appleby, P.G., 2008. Three decades of dating recent sediments by fallout radionuclides: a review. Holocene 18, 83–93. https://doi.org/10.1177/0959683607085598.

Appleby, P.G., Oldfield, F., 1978. The calculation of lead-210 dates assuming a constant rate of supply of unsupported 210Pb to the sediment. Catena 5, 1–8. https://doi.org/10.1016/S0341-8162(78)80002-2.

Appleby, P.G., Nolan, P.J., Gifford, D.W., Godfrey, M.J., Oldfield, F., Anderson, N.J., Battarbee, R.W., 1986. 210Pb dating by low background gamma counting. Hydrobiologia 143, 21–27.

Appleby, P.G., Richardson, N., Nolan, P.J., 1992. Self-absorption corrections for well-type germanium detectors. Nucl. Instruments Methods Phys. Res. Sect. B Beam Interact. with Mater. Atoms 71, 228–233.

Arias-Ortiz, A., Masqué, P., Garcia-Orellana, J., Serrano, O., Mazarrasa, I., Marbà, N., Lovelock, C.E., Lavery, P., Duarte, C.M., 2018. Reviews and syntheses: 210Pb-derived sediment and carbon accumulation rates in vegetated coastal ecosystems: setting the record straight. Biogeosci. Discuss. 15, 6791–6818. https://doi.org/10.5194/bg-2018-78.

Barnes, D.K.A., Galgani, F., Thompson, R.C., Barlaz, M., 2009. Accumulation and fragmentation of plastic debris in global environments. Philos. Trans. R. Soc. B Biol. Sci. 364, 1985–1998. https://doi.org/10.1098/rstb.2008.0205.

Barrows, A.P.W., Cathey, S.E., Petersen, C.W., 2018. Marine environment microfiber contamination: global patterns and the diversity of microparticle origins. Environ. Pollut. 237, 275–284. https://doi.org/10.1016/j.envpol.2018.02.062.

Bergmann, M., Wirzberger, V., Krumpen, T., Lorenz, C., Primpke, S., Tekman, M.B., Gerdts, G., 2017. High quantities of microplastic in Arctic deep-sea sediments from the HAUSGARTEN observatory. Environ. Sci. Technol. 51, 11000–11010. https://doi.org/10.1021/acs.est.7b03331.

Blott, S.J., Pye, K., 2001. GRADISTAT: a grain size distribution and statistics package for the analysis of unconsolidated sediments. Earth Surf. Process. landforms 26, 1237–1248.

Boonyatumanond, R., Wattayakorn, G., Amano, A., Inouchi, Y., Takada, H., 2007. Reconstruction of pollution history of organic contaminants in the upper gulf of Thailand by using sediment cores: first report from tropical Asia Core (TACO) project. Mar. Pollut. Bull. 54, 554–565. https://doi.org/10.1016/j.marpolbul.2006.12.007.

Bour, A., Avio, C.G., Gorbi, S., Regoli, F., Hylland, K., 2018. Presence of microplastics in benthic and epibenthic organisms: influence of habitat, feeding mode and trophic level. Environ. Pollut. 243, 1217–1225. https://doi.org/10.1016/j.envpol.2018.09.115.

Brandon, J.A., Jones, W., Ohman, M.D., 2019. Multidecadal increase in plastic particles in coastal ocean sediments. Sci. Adv. 5, eaax0587. https://doi.org/10.1126/sciadv.aax0587.

Browne, M.A., Crump, P., Niven, S.J., Teuten, E., Tonkin, A., Galloway, T., Thompson, R., 2011. Accumulation of microplastic on shorelines woldwide: sources and sinks. Environ. Sci. Technol. 45, 9175–9179. https://doi.org/10.1021/es201811s.

Bryan, G.W., Langston, W.J., 1992. Bioavailability, accumulation and effects of heavy metals in sediments with special reference to United Kingdom estuaries: a review. Environ. Pollut. 76, 89–131. https://doi.org/10.1016/0269-7491(92)90099-V.

Chant, L.A., Cornett, R.J., 1987. Smearing of gravity core profiles in soft sediments. Limnol. Oceanogr. 36, 1492–1498.

Claessens, M., De Meester, S., Van Landuyt, L., De Clerck, K., Janssen, C.R., 2011. Occurrence and distribution of microplastics in marine sediments along the Belgian coast. Mar. Pollut. Bull. 62, 2199–2204. https://doi.org/10.1016/j.marpolbul.2011.06.030.

Clunies-Ross, P.J., Smith, G.P.S., Gordon, K.C., Gaw, S., 2016. Synthetic shorelines in New Zealand? Quantification and characterisation of microplastic pollution on Canterbury's coastlines. New Zeal. J. Mar. Freshw. Res. 50, 317–325. https://doi.org/10.1080/00288330.2015.1132747.

Courtene-Jones, W., Quinn, B., Gary, S.F., Mogg, A.O.M., Narayanaswamy, B.E., 2017. Microplastic pollution identified in deep-sea water and ingested by benthic invertebrates in the Rockall trough, North Atlantic Ocean. Environ. Pollut. 231, 271–280. https://doi.org/10.1016/j.envpol.2017.08.026.

Courtene-Jones, W., Quinn, B., Ewins, C., Gary, S.F., Narayanaswamy, B.E., 2019. Consistent microplastic ingestion by deep-sea invertebrates over the last four decades (1976–2015), a study from the north East Atlantic. Environ. Pollut. 244, 503–512. https://doi.org/10.1016/j.envpol.2018.10.090.

Crichton, E.M., Noel, M., Gies, E.A., Ross, P.S., 2017. A novel, density-independent and FTIR-compatible approach for the rapid extraction of microplastics from aquatic sediments. Anal. Methods 9, 1419–1428. https://doi.org/10.1039/C6AY02733D.

Davies, A.J., Narayanaswamy, B.E., Hughes, D.J., Murray, J., 2006. An Introduction to the Benthic Ecology of the Rockall-Hatton Area. (SEA 7).

Fischer, V., Elsner, N.O., Brenke, N., Schwabe, E., Brandt, A., 2015. Plastic pollution of the Kuril–Kamchatka trench area (NW pacific). Deep Sea Res. Part II Top. Stud. Oceanogr. 111, 399–405. https://doi.org/10.1016/j.dsr2.2014.08.012.

Folk, R.L., Ward, W.C., 1957. River bar: a study in the significance of grain size parameters. J. Sediment. Petrol. 27, 3–26.

Frias, J.P.G.L., Gago, J., Otero, V., Sobral, P., 2016. Microplastics in coastal sediments from southern Portuguese shelf waters. Mar. Environ. Res. 114, 24–30. https://doi.org/10.1016/j.marenvres.2015.12.006.

Gage, J.D., 1986. The benthic fauna of the Rockall trough: regional distribution and bathymetric zonation. Proc. R. Soc. Edinburgh 88, 159–174. https://doi.org/10.1017/S026972700000453X.

Gage, J.D., Lightfoot, R.H., Pearson, M., Tyler, P.A., 1980. An introduction to a sample time-series of abyssal macrobenthos: methods and principle sources of variability. Oceanol. Acta 3, 169–176.

Gehlen, M., Rabouille, C., Ezat, U., Guidi-Guilvard, L.D., 1997. Drastic changes in deep-sea sediment porewater composition induced by episodic input of organic matter. Limnol. Oceanogr. 42, 980–986. https://doi.org/10.4319/lo.1997.42.5.0980.

Graham, E.R., Thompson, J.T., 2009. Deposit- and suspension-feeding sea cucumbers (Echinodermata) ingest plastic fragments. J. Exp. Mar. Bio. Ecol. 368, 22–29. https://doi.org/10.1016/j.jembe.2008.09.007.

Hardesty, B.D., Harari, J., Isobe, A., Lebreton, L., Potemra, J.T., Sebille, V., Vethaak, D., Wilcox, C., 2017. Using numerical model simulations to improve the understanding of micro-plastic distribution and pathways in the marine environment. Front. Mar. Sci. 4, 1–9. https://doi.org/10.3389/fmars.2017.00030.

Haywood, P.J., Ryland, J.S., 1990. The Marine Fauna of the British Isles and North-West Europe. Introduction and Protozoans to Arthropods Volume 1 Oxford University Press.
Holliday, N.P., Cunningham, S., Johnson, C., Gary, S.F., Griffiths, C., Read, J.F., Sherwin, T., 2015. Multidecadal variability of potential temperature, salinity, and transport in the eastern subpolar North Atlantic. J. Geophys. Res. Ocean. 120, 5945–5967. https://doi.org/10.1002/2014JC010472. Received.
Hong, G.-H., Hamilton, T.F., Baskaran, M., Kenna, T.C., 2011. Applications of anthropogenic radionuclides as tracers to investigate marine environmental processes. In: Baskaran, M. (Ed.), Handbook of Environmental Isotope Chemistry. Springer Berlin Heidelberg, pp. 367–394. https://doi.org/10.1007/978-3-642-10637-8_19.
Howe, J.A., 1995. Sedimentary processes and variations in slope-current activity during the last glacial-interglacial episode on the Hebrides slope, northern Rockall trough, North Atlantic Ocean. Sediment. Geol. 96, 201–230. https://doi.org/10.1016/0037-0738(94)00121-A.
Hu, Q.H., Weng, J.Q., Wang, J.S., 2010. Sources of anthropogenic radionuclides in the environment: a review. J. Environ. Radioact. 101, 426–437. https://doi.org/10.1016/j.jenvrad.2008.08.004.
Hughes, D.J., Brown, L., Cook, G.T., Cowie, G., Gage, J.D., Good, E., Kennedy, H., MacKenzie, A.B., Papadimitriou, S., Shimmield, G.B., Thomson, J., Williams, M., 2005. The effects of megafaunal burrows on radiotracer profiles and organic composition in deep-sea sediments: preliminary results from two sites in the bathyal north-East Atlantic. Deep. Res. Part I Oceanogr. Res. Pap. 52, 1–13. https://doi.org/10.1016/j.dsr.2004.09.006.
Jamieson, A.J., Boorman, B., Jones, D.O.B., 2013. Deep-sea benthic sampling. In: Eleftheriou, A. (Ed.), Methods for the Study of Marine Benthos. John Wiley & Sons Ltd, pp. 285–347. https://doi.org/10.1002/9781118542392.ch7.
Jamieson, A.J., Brooks, L.S.R., Reid, W.D.K., Piertney, S.B., Narayanaswamy, B.E., Linley, T.D., 2019. Microplastics and synthetic particles ingested by deep-sea amphipods in six of the deepest marine ecosystems on Earth. R. Soc. Open Sci. 6, 180667. https://doi.org/10.1098/rsos.180667.
Kane, I.A., Clare, M.A., 2019. Dispersion, accumulation, and the ultimate fate of microplastics in deep-marine environments: a review and future directions. Front. Earth Sci. 7. https://doi.org/10.3389/feart.2019.00080.
Kanhai, L.D.K., Johansson, C., Frias, J.P.G.L., Gardfeldt, K., Thompson, R.C., O'Connor, I., 2019. Deep sea sediments of the Arctic Central Basin: a potential sink for microplastics. Deep. Res. Part I Oceanogr. Res. Pap. 145, 137–142. https://doi.org/10.1016/j.dsr.2019.03.003.
Kirchner, G., 2011. Pb as a tool for establishing sediment chronologies : examples of potentials and limitations of conventional dating models. J. Environ. Radioact. 102, 490–494. https://doi.org/10.1016/j.jenvrad.2010.11.010.
Koelmans, A.A., Kooi, M., Law, K.L., Sebille, E. Van, Quality, W., Group, M., Hole, W., 2017. All is not lost: deriving a top-down mass budget of plastic at sea. Environ. Res. Lett. 12, 114028. https://doi.org/10.1088/1748-9326/aa9500.
Komárek, M., Ettler, V., Chrastný, V., Mihaljevič, M., 2008. Lead isotopes in environmental sciences: a review. Environ. Int. 34, 562–577. https://doi.org/10.1016/j.envint.2007.10.005.
Lwanga, E.H., Gertsen, H., Gooren, H., Peters, P., Salánki, T., van der Ploeg, M., Besseling, E., Koelmans, A.A., Geissen, V., 2017. Incorporation of microplastics from litter into burrows of Lumbricus terrestris. Environ. Pollut. 220, 523–531. https://doi.org/10.1016/j.envpol.2016.09.096.
MacKenzie, A.B., Hardie, S.M.L., Farmer, J.G., Eades, L.J., Pulford, I.D., 2011. Analytical and sampling constraints in 210Pb dating. Sci. Total Environ. 409, 1298–1304. https://doi.org/10.1016/j.scitotenv.2010.11.040.
Maes, T., Barry, J., Leslie, H.A., Vethaak, A.D., Nicolaus, E.E.M., Law, R.J., Lyons, B.P., Martinez, R., Harley, B., Thain, J.E., 2018. Below the surface: twenty-five years of seafloor litter monitoring in coastal seas of North West Europe (1992–2017). Sci. Total Environ. 630, 790–798. https://doi.org/10.1016/j.scitotenv.2018.02.245.
Martin, J., Lusher, A., Thompson, R.C., Morley, A., 2017. The deposition and accumulation of microplastics in marine sediments and bottom water from the Irish continental shelf. Sci. Rep. 7, 1–9. https://doi.org/10.1038/s41598-017-11079-2.
Masson, D.G., Howe, J.A., Stoker, M.S., 2002. Bottom-current sediment waves, sediment drifts and contourites in the northern Rockall trough. Mar. Geol. 192, 215–237. https://doi.org/10.1016/S0025-3227(02)00556-X.
Matsuguma, Y., Takada, H., Kumata, H., Kanke, H., Sakurai, S., Suzuki, T., Itoh, M., Okazaki, Y., Boonyatumanond, R., Zakaria, M.P., Weerts, S., Newman, B., 2017. Microplastics in sediment cores from Asia and Africa as indicators of temporal trends in plastic pollution. Arch. Environ. Contam. Toxicol. 73, 230–239. https://doi.org/10.1007/s00244-017-0414-9.
Michels, J., Stippkugel, A., Lenz, M., Wirtz, K., Engel, A., 2018. Rapid aggregation of biofilm-covered microplastics with marine biogenic particles. Proc. R. Soc. B Biol. Sci. 285, 20181203. https://doi.org/10.1098/rspb.2018.1203.
Näkki, P., Setälä, O., Lehtiniemi, M., 2017. Bioturbation transports secondary microplastics to deeper layers in soft marine sediments of the northern Baltic Sea. Mar. Pollut. Bull. 119, 255–261. https://doi.org/10.1016/j.marpolbul.2017.03.065.
Narayanaswamy, B.E., Bett, B.J., Lamont, P.A., Rowden, A.A., Bell, E.M., Menot, L., 2016. Corers and grabs. In: Clark, M.R., Consalvey, M., Rowden, A.A. (Eds.), Biological Sampling in the Deep Sea. Wiley Blackwell, pp. 207–227. https://doi.org/10.1002/9781118332535.ch10.
Oksanen, A.J., Blanchet, F.G., Friendly, M., Kindt, R., Legendre, P., McGlinn, D., Minchin, P.R., O'Hara, R.B., Simpson, G.L., Solymos, P., Henry, M., Stevens, H., Szoecs, E., Wagner, H., 2018. Community Ecology Package. (https://doi.org/ISBN 0-387-95457-0).
Paterson, G.L.J., Lambshead, P.J.D., 1995. Bathymetric patterns of polychaete diversity in the Rockall trough, Northeast Atlantic. Deep-Sea Res. 42 (7), 1199–1214 (4 figures, 2 tables. Deep Sea Res. Part I … 42, 1199–1214).
Peng, X., Chen, M., Chen, S., Dasgupta, S., Xu, H., Ta, K., Du, M., Li, J., Guo, Z., Bai, S., 2018. Microplastics contaminate the deepest part of the world's ocean. Geochemical Perspect. Lett. 9, 1–5. https://doi.org/10.1029/2003PA000923.
Porter, A., Lyons, B.P., Galloway, T.S., Lewis, C., 2018. Role of marine snows in microplastic fate and bioavailability. Environ. Sci. Technol. 52, 7111–7119. https://doi.org/10.1021/acs.est.8b01000.
Primpke, S., Wirth, M., Lorenz, C., Gerdts, G., 2018. Reference database design for the automated analysis of microplastic samples based on Fourier transform infrared (FTIR) spectroscopy. Anal. Bioanal. Chem. 410, 5131–5141. https://doi.org/10.1007/s00216-018-1156-x.
R Core Team, 2016. R: A Language and Environment for Statistical Computing. R Foundation for Statistical Computing.
Ramirez-Llodra, E., Brandt, A., Danovaro, R., De Mol, B., Escobar, E., German, C.R., Levin, L.A., Martinez Arbizu, P., Menot, L., Buhl-Mortensen, P., Narayanaswamy, B.E., Smith, C.R., Tittensor, D.P., Tyler, P.A., Vanreusel, A., Vecchione, M., 2010. Deep, diverse and definitely different: unique attributes of the world's largest ecosystem. Biogeosciences 7, 2851–2899. https://doi.org/10.5194/bg-7-2851-2010.
Reimers, C.E., Jahnke, R.A., McCorkle, D.C., 1992. Carbon fluxes and burial rates over the continental slope and rise off central California with implications for the global carbon cycle. Glob. Biogeochem. Cycles 6, 199–224. https://doi.org/10.1029/92GB00105.
Sanchez-Vidal, A., Thompson, R.C., Canals, M., de Haan, W.P., 2018. The imprint of microplastics from textiles in southern European deep seas. PLoS One 13, e0207033. https://doi.org/10.1371/journal.pone.0207033.
Sarkar, D., 2018. Trellis Graphics for R.
Scott, A., Penlidis, A., 2017. Copolymerization. In: Reference Module in Chemistry, Molecular Sciences and Chemical Engineering. Elsevier. https://doi.org/10.1016/B978-0-12-409547-2.13901-0.
Simpson, G.L., Team, R.C., Bates, D.M., Oksanen, J., 2016. Functions for Generating Restricted Permutations of Data.
Stolte, A., Forster, S., Gerdts, G., Schubert, H., 2015. Microplastic concentrations in beach sediments along the German Baltic coast. Mar. Pollut. Bull. 99, 216–229. https://doi.org/10.1016/j.marpolbul.2015.07.022.
Suess, E., 1980. Particulate organic carbon flux in the oceans- surface productivity and oxygen utilization. Nature 288, 260–263. https://doi.org/10.1038/288260a0.
Summers, S., Henry, T., Gutierrez, T., 2018. Agglomeration of nano- and microplastic particles in seawater by autochthonous and de novo-produced sources of exopolymeric substances. Mar. Pollut. Bull. 130, 258–267 (https://doi.org/S0025326X18302042).
Taylor, M.L., Gwinnet, C., Robinson, L.F., Woodall, L.C., 2016. Plastic microfibre ingestion by deep-sea organisms. Sci. Rep. 6, 1–9. https://doi.org/10.1038/srep33997.
Teal, L.R., Bulling, M.T., Parker, E.R., Solan, M., 2008. Global patterns of bioturbation intensity and mixed depth of marine soft sediments. Aquat. Biol. 2, 207–218. https://doi.org/10.3354/ab00052.
Thomson, J., Brown, L., Nixon, S., Cook, G.T., MacKenzie, A.B., 2000. Bioturbation and Holocene sediment accumulation fluxes in the north-East Atlantic Ocean (benthic boundary layer experiment sites). Mar. Geol. 169, 21–39. https://doi.org/10.1016/S0025-3227(00)00077-3.
Turner, S., Horton, A.A., Rose, N.L., Hall, C., 2019. A temporal sediment record of microplastics in an urban lake, London, UK. J. Paleolimnol. 61, 449–462. https://doi.org/10.1007/s10933-019-00071-7.
Van Cauwenberghe, L., Vanreusel, A., Mees, J., Janssen, C.R., 2013. Microplastic pollution in deep-sea sediments. Environ. Pollut. 182, 495–499. https://doi.org/10.1016/j.envpol.2013.08.013.
Van Cauwenberghe, L., Devriese, L., Galgani, F., Robbens, J., Janssen, C.R., 2015. Microplastics in sediments: a review of techniques, occurrence and effects. Mar. Environ. Res. 111, 5–17. https://doi.org/10.1016/j.marenvres.2015.06.007.
Van Metre, P., Mahler, B.J., 2005. Trends in hydrophobic organic contaminants in urban and reference lake sediments across the United States, 1970-2001. Environ. Sci. Technol. 39, 5567–5574. https://doi.org/10.1021/es0503175.
Warwick, P.E., Croudace, I.W., Oh, J.S., 2001. Radiochemical determination of 241Am and Pu(α) in environmental materials. Anal. Chem. 73, 3410–3416. https://doi.org/10.1021/ac001510e.
Wheatcroft, R.A., 1992. Experimental tests for particle size-dependent bioturbation in the deep ocean. Limnol. Oceanogr. 37, 90–104. https://doi.org/10.4319/lo.1992.37.1.0090.
Wichkham, H., Chang, W., 2016. Package 'ggplot 2.'.
Willis, K.A., Eriksen, R., Wilcox, C., Hardesty, B.D., 2017. Microplastic distribution at different sediment depths in an urban estuary. Front. Mar. Sci. 4, 419. https://doi.org/10.3389/fmars.2017.00419.
Woodall, L.C., Sanchez-Vidal, A., Canals, M., Paterson, G.L.J., Coppock, R., Sleight, V., Calafat, A., Rogers, a.D., Narayanaswamy, B.E., Thompson, R.C., 2014. The deep sea is a major sink for microplastic debris. R. Soc. Open Sci. 1, 140317. https://doi.org/10.1098/rsos.140317.